

UNCLASSIFIED

**Defense Technical Information Center  
Compilation Part Notice**

**ADP012608**

**TITLE:** Lead Telluride-based Far-infrared Photodetectors. A Promising Alternative to Doped Si and Ge

**DISTRIBUTION:** Approved for public release, distribution unlimited

**This paper is part of the following report:**

**TITLE:** Progress in Semiconductor Materials for Optoelectronic Applications Symposium held in Boston, Massachusetts on November 26-29, 2001.

**To order the complete compilation report, use: ADA405047**

The component part is provided here to allow users access to individually authored sections of proceedings, annals, symposia, etc. However, the component should be considered within the context of the overall compilation report and not as a stand-alone technical report.

The following component part numbers comprise the compilation report:  
ADP012585 thru ADP012685

UNCLASSIFIED

### **Lead telluride-based far-infrared photodetectors – a promising alternative to doped Si and Ge.**

Dmitriy Dolzhenko, Ivan Ivanchik, Dmitriy Khokhlov, Konstantin Kristovskiy  
Physics Department, Moscow State University, Moscow 119899, Russia

#### **ABSTRACT**

Doping of the lead telluride and related alloys with the group III impurities results in appearance of unique physical features of the material, such as persistent photoresponse, enhanced responsive quantum efficiency (up to 100 photoelectrons/incident photon), radiation hardness and many others. We review physical principles of operation of the photodetecting devices based on the group III-doped IV-VI including possibilities of fast quenching of the persistent photoresponse, construction of a focal-plane array, new readout technique, and others. Comparison of performance of the state of the art Ge(Ga) and Si(Sb) photodetectors with their lead telluride-based analogs shows that the responsivity of PbSnTe(In) photodetectors is by several orders of magnitude higher. High photoresponse is detected at the wavelength 116 micrometers in PbSnTe(In), and it is possible that the photoconductivity spectrum covers all the submillimeter wavelength range.

#### **INTRODUCTION**

Many of the sensitive photodetecting systems operating in the far infrared wavelength range (20-200)  $\mu\text{m}$  are based on germanium or silicon doped with shallow impurities [1]. The highest cut off wavelength reported  $\lambda_{\text{co}} \approx 220 \mu\text{m}$  corresponds to the uniaxially stressed Ge(Ga) [2]. The main advantage of germanium and silicon is very well developed growth technology that allows receiving materials with perfect crystalline quality and extremely low uncontrolled impurity concentration.

An alternative possibility for construction of sensitive far-infrared photodetectors is provided by unique features of a narrow-gap semiconductor - indium-doped  $\text{Pb}_{1-x}\text{Sn}_x\text{Te}$ . Exciting results of fundamental research on the group III - doped lead telluride - based alloys [3] provided possibilities for construction of far-infrared photodetectors based on new physical principles [4]. Results of these activities are very promising since performance of far-infrared photodetectors based on doped lead-tin tellurides is comparable or better than for analogs based on doped Ge or Si.

#### **INDIUM-DOPED LEAD-TIN TELLURIDES: THE MAIN PROPERTIES**

##### **Fermi level pinning.**

Doping of the lead telluride with indium in amount exceeding concentration of other impurities and defects results in the Fermi level pinning effect [5]. A consequence of this effect is homogenization of electrical properties of the semiconductor. This feature results in almost absolute reproducibility of sample parameters independently on the growth technology. High sample homogeneity gives rise to enhanced carrier mobility reaching  $10^5$ - $10^6 \text{ cm}^2/\text{V}\cdot\text{s}$  at low temperatures.

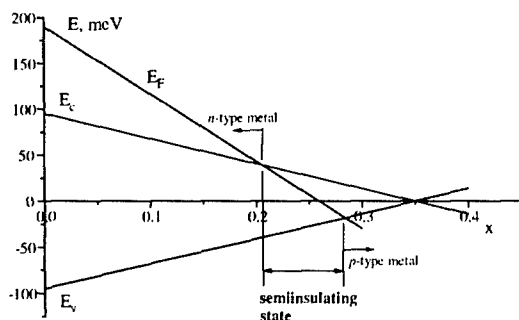


**Figure 1.** Energy diagram of the  $\text{Pb}_{1-x}\text{Sn}_x\text{Te(In)}$  alloys for different  $x$ .  $E_c$  - conduction band bottom,  $E_v$  - valence band [6].

Position of the pinned Fermi level  $E_0$  may be tuned by alloying (Figure 1) [6]. It crosses the gap in the tin content range ( $0.22 < x < 0.28$ ) providing the semiinsulating state of the semiconductor for this range of alloy compositions. Conductivity of material in the semiinsulating state ( $0.22 < x < 0.28$ ) is defined by activation from the impurity local level  $E_0$ , and therefore the free carrier concentration is very low  $n, p < 10^8 \text{ cm}^{-3}$  at temperatures  $T < 10 \text{ K}$ . The free carrier concentration in undoped alloys is defined by electrically active growth defects. Their concentration is never less than  $10^{15} \text{ cm}^{-3}$ . So we have a very unusual situation, when a heavily doped narrow-gap semiconductor with high number of growth defects acts as an almost ideal semiconductor with practically zero background free carrier concentration and very high electrical homogeneity. This makes very attractive the idea to use this material as an infrared photodetector.

### **Persistent photoconductivity.**

External infrared illumination leads to the substantial increment of material conductivity at the temperatures  $T < 25 \text{ K}$  (Figure 2) [7]. High amplitude of photoresponse at the low temperatures is a consequence of the persistent photoconductivity effect: the photoresponse increases linearly in time providing a kind of «internal integration» of the incident radiation flux. When the radiation is switched off, the conductivity relaxes very slowly. The characteristic relaxation time  $\tau > 10^4 \text{ s}$  at  $4.2 \text{ K} < T < 10 \text{ K}$ , then it sharply decreases with the temperature rising, and  $\tau \sim 10^{-2} \text{ s}$  at  $T \approx 20 \text{ K}$ . The effect is defined by the specifics of impurity states that form DX-like centers [8].

If sample temperature is so that  $\tau$  is higher than the operation time required, then a photoresistor may operate only if there exists a possibility to return to the initial "darkness" state, i.e. to quench quickly the persistent photoconductivity. Moreover, periodical accumulation and successive fast quenching of the photosignal leads to the substantial gain in the S/N ratio with respect to the case of ordinary single photodetectors. The most efficient way of quenching of the

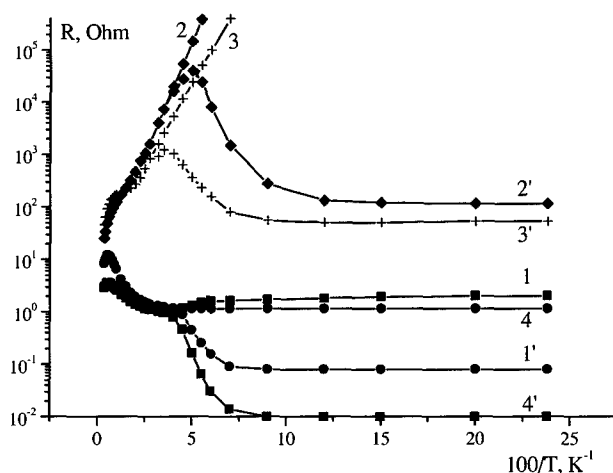


**Figure 2.** Temperature dependence of the sample resistance  $R$  measured in darkness (1-4) and under infrared illumination (1'-4') in alloys with  $x = 0.22$  (1, 1'), 0.26 (2, 2'), 0.27 (3, 3') and 0.29 (4, 4') [7].

persistent photoconductivity in  $\text{Pb}_{1-x}\text{Sn}_x\text{Te(In)}$  is application of strong microwave pulses to sample contacts [4]. Using this technique the long-living photoexcited free electrons may be localized for 10  $\mu\text{s}$ . Therefore it became possible to operate in the regime of periodical accumulation and successive fast quenching of photoresponse. Moreover, application of microwave pulses in some special regime results in giant increment of the quantum efficiency up to  $\sim 100$  [4].

### Radiometric parameters.

A laboratory model of the IR-radiometer based on  $\text{Pb}_{1-x}\text{Sn}_x\text{Te(In)}$  operating in the regime of periodical accumulation and successive fast quenching of the persistent photoconductivity, has been demonstrated in [4]. A helium-cooled grid filter provided effective cutting of the incident radiation spectrum at the wavelengths  $\lambda > 18 \mu\text{m}$ . Despite low sensitivity of the measuring electronics used, the photon flux detected in [4] was as low as  $N \approx 2 \cdot 10^4 \text{ s}^{-1}$  that corresponds to  $\text{NEP} \approx 2 \cdot 10^{-16} \text{ W}$  for the detector area of  $0.3 \cdot 0.2 \text{ mm}^2$  and the operating rate 3 Hz.

Direct comparison of the  $\text{Pb}_{0.75}\text{Sn}_{0.25}\text{Te(In)}$  photodetector, the Si(Sb) BIB structure and the Ge(Ga) photodetector using the same cryogenic equipment and measuring electronics has been performed in [9]. The responsivity  $S_1$  of the  $\text{Pb}_{0.75}\text{Sn}_{0.25}\text{Te(In)}$  photodetector at  $116 \mu\text{m}$  was of the order of  $10^3 \text{ A/W}$  at 40 mV bias, that is by 2-3 orders of magnitude higher than the  $S_1$  value obtained for a state of the art Ge(Ga) photodetector in the same measuring conditions.

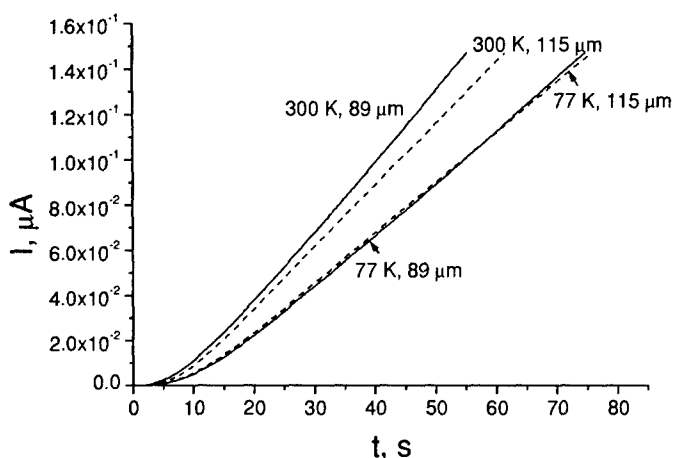


**Figure 3.** Photoconductivity kinetics of  $\text{Pb}_{0.75}\text{Sn}_{0.25}\text{Te}(\text{In})$  film exposed to blackbody radiation filtered at  $\lambda = 90$  and  $116 \mu\text{m}$ . Figures - the blackbody temperature and the wavelength.  $T = 4.2$  K. Illumination starts at the moment  $t = 0$  (with accuracy of (3-4) s) [9].

The same authors have directly observed persistent photoresponse in the  $\text{Pb}_{0.75}\text{Sn}_{0.25}\text{Te}(\text{In})$  photodetector at the wavelengths of 90 and  $116 \mu\text{m}$  (Figure 3) that are considerably longer than the wavelength corresponding to the thermal activation energy of the ground impurity state. Indications exist that the red cutoff wavelength for this photodetector may exceed  $220 \mu\text{m}$  - the highest  $\lambda_{\text{co}}$  observed so far.

#### **"Continuous" focal-plane array.**

Specifics of impurity states may make very easy construction of a focal-plane array on  $\text{Pb}_{1-x}\text{Sn}_x\text{Te}(\text{In})$ . Local infrared illumination leads to local generation of nonequilibrium free electrons, i.e. the persistent photoconductivity effect is observed only in the illuminated part of the sample, and the photoexcitation does not propagate into the darkened regions [10]. The characteristic time of the excitation propagation is at least more than  $10^4$  s at  $T = 4.2$  K. The spatial characteristic scale is  $\sim 10 \mu\text{m}$ . The physical picture of the processes involved is the following. The photoexcited free electrons cannot diffuse far away from the region of generation due to electrostatic attraction to the ionized impurity centers. On the other hand these electrons cannot recombine because of the existence of a barrier between the local and extended states.

Therefore the distribution of the radiation exposure over the sample surface reflects in a distribution of the concentration of long-living free electrons. In other words, it is possible to construct a focal plane "continuous" array, in which the signal is internally integrated in every effective element.

Readout technique is a special problem. The approach proposed in [4] seems to be the most promising. Let us consider a thin slice of  $\text{Pb}_{1-x}\text{Sn}_x\text{Te}(\text{In})$  with a semitransparent electrode

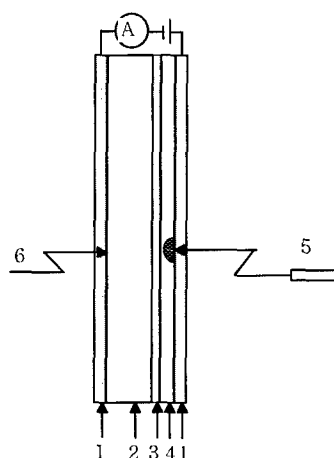


**Figure 4.** Device for readout of information from the "continuous" focal-plane array on  $\text{Pb}_{1-x}\text{Sn}_x\text{Te(In)}$ . 1 - semitransparent electrodes, 2 - active  $\text{Pb}_{1-x}\text{Sn}_x\text{Te(In)}$  layer, 3 - fluoride buffer layer, 4 - layer of a silicon (or other semiconductor with a relatively wide gap), 5 - short-wavelength laser, 6 - incident infrared radiation flux [4].

deposited on one side (Figure 4). The investigated radiation flux illuminates the sample from the same left side in the Figure 4. A buffer insulating fluoride layer is deposited on another side of the sample followed by a thin layer of silicon or some other semiconductor with a relatively wide gap, and a second semitransparent electrode. If the sample is illuminated by a shortwavelength laser from the right side (see Figure 4), it is possible to generate a local highly conductive region in the wide-gap semiconductor. If then a bias between the electrodes is applied, the current is defined by the  $\text{Pb}_{1-x}\text{Sn}_x\text{Te(In)}$  sample conductivity in the region of the laser spot, because the thickness of the semiinsulating wide-gap semiconductor layer is be much less in this point. Another advantage of such a readout technique is heavy damping of the dark current in such a structure. It is analogous to certain extent to the ideas involved in BIB structures. If the recombination rate in the wide-gap semiconductor is high enough, it is easy to reconstruct the conductivity distribution over the  $\text{Pb}_{1-x}\text{Sn}_x\text{Te(In)}$  sample simply by scanning the laser beam over the structure surface and by measuring the respective current. Unfortunately this idea is not realized in practice so far.

### **Radiation hardness.**

High radiation hardness is one more advantage of the photodetectors based on  $\text{Pb}_{1-x}\text{Sn}_x\text{Te(In)}$ . This is a consequence of a very high density of impurity states ( $\sim 10^{18} - 10^{19} \text{ cm}^{-3}$ ) that pin the Fermi level. The fast electron irradiation with fluencies up to  $10^{17} - 10^{18} \text{ cm}^{-2}$  does not affect the photoresponse [11]. This value is at least by 4 orders of magnitude higher than for  $\text{Hg}_{1-x}\text{Cd}_x\text{Te}$ , doped Ge and Si.

## SUMMARY

In summary, application of the lead-tin tellurides doped with the group III impurities as base elements for the infrared photodetectors gives a challenging opportunity to produce universal and sensitive systems. They have a number of advantageous features that allow them to compete successfully with the existing analogs: internal accumulation of the incident radiation flux, possibility of effective fast quenching of an accumulated signal, microwave stimulation of the quantum efficiency up to  $10^2$ , possibility of realization of a "continuous" focal-plane array, possibility of application of a new readout technique, high radiation hardness. In our opinion, these features make the  $\text{Pb}_{1-x}\text{Sn}_x\text{Te(In)}$ -based photodetectors ideal for the space-borne applications, for example, in the infrared astronomy.

## ACKNOWLEDGMENTS

The research described in this paper was supported in part by the grant of the Russian Foundation for the Basic Research (RFBR) No. 01-02-16356.

## REFERENCES

1. J.Wolf and D.Lemke, *Infrared Phys.* **25**, 327 (1985).
2. E.E.Haller, M.R.Hueschen and P.L.Richards, *Appl. Phys. Lett.* **34**, 495 (1979).
3. B.A.Akimov, A.V.Dmitriev, D.R.Khokhlov, and L.I.Ryabova, *Phys. Stat. Sol. A*: **137**, 9 (1993).
4. S.N.Chesnokov, D.E.Dolzhenko, I.I.Ivanchik, and D.R.Khokhlov, *Infrared Phys.* **35**, 23 (1994).
5. V.I.Kaidanov, R.B.Mel'nik, and I.A.Chernik, *Fiz. Tekh. Poluprov.* **7**, 759 (1973) [*Sov. Phys. Semicond.* **7**, 522 (1973)].
6. B.A.Akimov, L.I.Ryabova, O.B.Yatsenko, and S.M.Chudinov, *Fiz. Tekh. Poluprovodn.* **13**, 752 (1979) [*Sov. Phys. Semicond.* **13**, 441 (1979)].
7. B.M.Vul, I.D.Voronova, G.A.Kaluzhnaya, T.S.Mamedov, and T.Sh.Ragimova, *Pis'ma v Zh.Eksp.Teor.Fiz.* **29**, 21 (1979); B.A.Akimov, N.B.Brandt, S.O.Klimonskiy, L.I.Ryabova, and D.R.Khokhlov, *Phys.Lett.* **88A**, 483 (1982).
8. D.R.Khokhlov and B.A.Volkov, *Proc. 23 Int. Conf. Phys. Semicond.*, Berlin, Germany, July 21-26, 1996, ed. M.Scheffer, R.Zimmermann, World Sci. (Singapore), **4**, 2941 (1996).
9. D.R.Khokhlov, I.I.Ivanchik, S.N.Raines, D.M.Watson, and J.L.Pipher, *Appl. Phys. Lett.* **76**, 2835 (2000).
10. B.A.Akimov, N.B.Brandt, S.N.Chesnokov, K.N.Egorov and D.R.Khokhlov, *Solid State Commun.* **66**, 811 (1988).
11. E.P.Skipetrov, A.N.Nekrasova, and A.G.Khorosh, *Fiz. Tekh. Poluprovodn.* **28**, 815 (1994) [*Sov. Phys. Semicond.* **28**, 478 (1994)].